J. Biochem. 2009;145(4)451–459
doi:10.1093/jb/mvn182

Highly Active Low Magnesium Hammerhead Ribozyme

Agnieszka Fedoruk-Wyszomirska*, Maciej Szymański*, Eliza Wyszko, Mirosława Z. Barciszewska and Jan Barciszewski†

Institute of Bioorganic Chemistry, Polish Academy of Sciences, Noskowskiego 12/14, 61-704 Poznań, Poland

Received October 28, 2008; accepted December 19, 2008; published online January 4, 2009

Hammerhead (HH) ribozymes can be used for highly specific inhibition of gene expression through the degradation of target mRNA. *In vitro* experiments with minimal HH domains demonstrated that the efficiency of catalysis is highly dependent on concentration of magnesium ions. Optimal ion requirements for HH-catalysed RNA cleavage are far from these found in the cell. Recently, it has been proposed that the efficiency of HH ribozymes can be increased at low magnesium concentration through stabilization of a catalytically active conformation by tertiary interactions between helices I and II. We designed a ribozyme stabilized by GAAA tetraloop and its receptor motifs and demonstrated that it can efficiently catalyse target RNA hydrolysis at submillimolar Mg^{2+} concentrations *in vitro* as well as in cultured cells. Both unmodified and locked nucleic acid-modified extended ribozymes proved superior to the minimal core ribozyme and DNAzyme against the same target sequence.

Key words: DNAzyme, hammerhead ribozyme, HIV, RNA, tetraloop receptor.

Abbreviations: HH, hammerhead; TL, tetraloop; TLR, tetraloop receptor.

Ribozymes are a class of biomolecules that have been in the focus of RNA research for >20 years. The studies on ribonuclease P RNA and self-splicing introns demonstrated that RNA molecules could act as efficient catalysts in biological systems (*1*, *2*). Subsequent discovery of hammerhead (HH) ribozymes capable of sequence-specific cleavage of RNA brought about the ideas of their application as 'catalytic antisense' tools for disruption of viral RNAs (*3*, *4*).

The action of ribozyme against a specific RNA sequence is a combination of a sense–antisense base pairing of nucleic acids (*5*) and a catalytic hydrolysis of the target (*6*). The HH ribozyme is the smallest of the naturally occurring catalytic RNAs identified to date (*7*, *8*). The natural HH ribozymes are *cis*-acting RNA motifs responsible for the self-cleavage of viroid genomic RNAs. It is, however, possible to separate the catalytic core that can act in *trans* and cleave target RNAs. The *trans*-acting HH ribozymes recognize their targets with high specificity due to sequence complementarity between the nucleotides flanking the ribozyme's catalytic core and the cleavage site. Usually, the target sequence is 13–14 nucleotides long and ensures high specificity of the ribozyme binding.

The development of HH ribozyme variants that cleave target RNA molecules in *trans* (*9*) was a major breakthrough that lay foundations for the practical application of ribozyme technology (*10–12*). The only requirement is a presence of an NUH (N—any nucleotide, H—A, C or U) triplet at the cleavage site. Efficient *trans*-acting ribozymes can be employed to decrease or abolish the expression of target genes. Extensive studies carried out over the last two decades confirmed their potential as anti-viral factors including their application against human immunodeficiency virus (HIV) (*13–17*). Ribozymes may represent useful therapeutic tool to avoid, in the long term, the emergence of drug-resistant viral populations and have the possibility of interfering with different stages of the viral life cycle (*17*).

One of the potential targets for anti-HIV therapy is the viral envelope glycoprotein gp41 that together with gp120, plays an essential role in HIV infection (*18*, *19*) and host cell tropism (*20*) controlling the entry of HIV into target cells. Moreover, the gp41 plays an important role in immunosuppression and immune dysfunction associated with HIV-infection (*21*, *22*) and disease progression (*23–26*). The effects of gp41 on the host immune system includes induction of the release of proinflammatory cytokines (TNF-α and IL-1) (*27*, *28*), suppression of lymphocyte proliferation (*29*), up-regulation of interleukin 10 (IL-10) synthesis in peripheral blood mononuclear cells (PBMC) and monocytes and down-regulation of the of IL-2 and interferon-γ (IFN-γ) production (*30*, *31*). The gp41 has been also detected in brain tissues of patients affected by AIDS dementia (*32*) where it is responsible for the induction of IL-10 synthesis by astrocytes and neurons (*33*).

The most fundamental problem with the application of *trans*-acting minimal HH ribozymes *in vitro* is their strong dependence on relatively high concentration of magnesium ions to achieve high catalytic activity. In the *in vitro* studies, the highest efficiency of HH ribozyme-catalysed RNA cleavage is observed in the presence of 10 mM Mg^{2+} (*6*). On the other hand, concentration of Mg^{2+} in cells varies between 0.4 and 0.8 mM depending on tissue type and physiological state (*34–36*).

*These authors contributed equally to this work.
†To whom correspondence should be addressed. Tel: +48-61-8528503, Fax: +48-61-8530523,
E-mail: jan.barciszewski@ibch.poznan.pl

Low concentration of magnesium in the cytoplasm may be a critical factor limiting the efficiency of HH ribozyme activity *in vivo*. The attempts to develop HH ribozyme variants with lowered requirement for Mg^{2+} included changes within the catalytic core and an addition of elements stabilizing active conformation of the ribozyme–substrate complex (*37*, *38*).

In this article, we present a new HH ribozyme stabilized by tertiary interactions between the GAAA tetraloop (TL) and a tetraloop receptor (TLR). The TL is a part of the standard minimal HH ribozyme, while the TLR-containing motif is embedded within the hairpin extension of the helix I at the 5′-end of the molecule. Target recognition elements of the ribozyme were designed to match the sequence of the mRNA encoding HIV-1 gp41. We show that, under low magnesium conditions, the ribozyme stabilized by TL–TLR interactions shows higher activity than the minimal ribozyme or a DNAzyme targeting the same region of gp41 gene. The efficiency of the new ribozyme was also demonstrated in the cultured cells where it was used to down-regulate expression of green fluorescent protein. Our results indicate that the stabilization of ribozyme structure by TL–TLR motifs can be used for the development of new effective anti-viral strategies.

MATERIALS AND METHODS

Oligonucleotides—HH ribozymes: HRz-gp41, TLR-HRz-gp41 and 25-nt long GUA target sequence (gp41-25; fragment of HIV-1 gp41 RNA corresponding to nucleotides 7375–7400; GenBank AccNo AF033819) were chemically synthesized by IBA GmbH, Göttingen, Germany. TLR-HRz-gp41 with locked nucleic acid (LNA) modifications was obtained from Eurogentec S.A., Seraing, Belgium. Anti-gp41 10-23 DNA enzyme (Dz-gp41) was purchased from the Institute of Biochemistry and Biophysics, Warsaw, Poland. Mutants of catalytic nucleic acids (MHRz-gp41, MTLR-HRz-gp41 and M-Dz-gp41) were transcribed using the Ambion megashortscript T7 transcription kit and synthetic DNA templates. RNA was purified on 10% PAGE with 7 M urea and eluted from gel slices in RNase-free water (Ambion). RNA was precipitated with 2.5 vol. of 96% ethanol in the presence of 0.1 vol. of 5 M ammonium acetate solution containing 100 mM EDTA (Ambion). The amount of RNA was calculated from the UV-absorbance measurements.

In vitro *Cleavage Assays by Ribozymes and DNAzyme*—The catalytic activities of HRz-gp41, TLR-HRz-gp41 and Dz-gp41 were analysed in 50 mM Tris–HCl buffer pH 7.5 at 25°C. Prior to the reaction the RNAs were denatured for 2 min at 85°C and slowly cooled down to 25°C (1°C/min). In the case of Dz-gp41, DNAzyme and substrate were denatured separately. The reactions were initiated by addition of $MgCl_2$ to a desired final concentration. All cleavage reactions were stopped by addition of equal volume of stop buffer (25 mM sodium citrate pH 5; 1 mM EDTA, 7 M urea; 0.1% xylene cyanol and 0.1% bromophenol blue), 2 μl 500 mM EDTA and by cooling on ice. Substrate and digestion products were separated on 20% polyacrylamide gels with 7 M urea in 0.09 M Tris–borate buffer pH 8.3.

Determination of Kinetic Parameters—To determine kinetic parameters of HRz-gp41, TLR-HRz-gp41, Dz-gp41 in excess of catalytic nucleic acids 10 nM of gp41-25 RNA substrate was mixed with 1 μM of HRz-gp41, TLR-HRz-gp41 or Dz-gp41. Reactions were carried out in 50 mM Tris–HCl, pH 7, denatured in 85°C for 3 min, then cooled slowly (1°C/min.) to the room temperature. After equilibrating at 25°C for 5 min, one-tenth of the sample was removed at a zero time point and quenched in an equal volume of stop buffer and 2 μl 500 mM EDTA. Reactions were initiated by adding $MgCl_2$ to the desired concentration. Aliquots were removed at 0.5, 1, 2.5, 5, 15, 30, 45 and 60 min and quenched with stop buffer. Reaction products were analysed on denaturing 20% polyacrylamide gels. K_{obs} values were calculated by fitting to $f_t = 1-\exp(k_{obs}t)$, where f_t is the fraction cleaved at time t. Reactions at substrate excess were carried out in similar manner using 10 nM of TLR-HRz-gp41 and 100 nM gp41-25. Aliquots were removed after 1, 5, 15, 30, 45, 60, 90, 120, 180 min and quenched in stop buffer.

Analysis of Catalytic Nucleic Acids Stability in HeLa Cell Extract—The 5×10^6 HeLa cells were sonicated 3×30 s (80 pulses, 70% amplitude) at regular 5 min intervals. The extract was diluted 50 times and used as an incubation medium for 5′-end labelled TLR-HRz-gp41, TLR-HRz-gp41$_{LNA}$ and DNAzyme to analyse their resistant to nucleases. Aliquots were removed after 5, 15, 30, 60, 120, 360 min and 24 h incubation at 37°C, and the integrity of nucleic acids was analysed on 20% denaturing polyacrylamide gels.

Assessment of Hydrolysis—The analysis of substrate (gp41-25) hydrolysis with catalytic nucleic acids was assessed using Typhoon 8600 Imager with ImageQuant software (Molecular Dynamics). The yield of hydrolysis is presented as a fraction of the substrate converted to product. Each point represents the mean ± SD for at least three independent measurements.

Radioactive Labelling of Target RNAs—For cleavage experiments with HH ribozymes and DNAzyme, 3–5 μg of target RNA gp41-25 were labelled at the 5′-end with 20 μCi of [γ-^{32}P]ATP (ICN), using 5U of T4 polynucleotide kinase (Amersham Pharmacia) for 30 min at 37°C in the 10× reaction buffer containing 0.5 M Tris–HCl pH 7.6, 100 mM $MgCl_2$ and 100 mM 2-mercaptoethanol (Amersham Pharmacia). The labelled target RNA was purified on 10% denaturing polyacrylamide gel. The radioactive band was excised and RNA was eluted 15 h with RNase-free water (Ambion) at room temperature, and precipitated with 2.5 vol. 96% ethanol in the presence of 0.1 vol. 5 M ammonium acetate with 100 mM EDTA (Ambion) and dissolved in RNase-free water. The amount of the labelled RNAs was calculated by scintillation counting.

Limited RNase Hydrolysis—The limited hydrolysis of labelled substrates (40,000 c.p.m.) with T1 RNase (Sigma) in denaturing conditions was done in 20 mM sodium acetate buffer, pH 4.5, containing 7 M urea and 1 mM EDTA for 20 min at 55°C, and 2 μg of total RNA from *Lupinus luteus* as a carrier. The reactions were stopped by addition of equal volume of loading buffer (25 mM sodium citrate pH 5; 1 mM EDTA; 7 M urea; 0.1% xylene cyanol and 0.1% bromophenol blue).

Alkaline Hydrolysis—To generate a sequence ladder RNA, alkaline hydrolysis of gp41-25 (40,000 c.p.m.) was performed at 99°C for 90 s in 10 µl of reaction mixture containing 50 mM NaOH, 1 mM EDTA and 4 µg of total RNA from *L. luteus* as a carrier. The reactions were stopped by addition of equal volume of loading buffer (25 mM sodium citrate pH 5; 1 mM EDTA; 7 M urea; 0.1% xylene cyanol and 0.1% bromophenol blue).

Plasmid Construct—Peripheral blood mononuclear cells (PBMCs) from HIV-1 positive donors were isolated by Ficoll-Hypaque gradient centrifugation and seeded at a density 1×10^6 cells per well in 4-well tissue culture plates. The cells were growing in RPMI 1640 medium (Sigma) supplemented with 10% fetal calf serum (FCS) at 37°C under a 5% CO_2 atmosphere in the absence of antibiotics. After 1 day of culture, adherent cells were gently washed, placed in fresh growth medium and incubated for 1 week. Total RNA including HIV-1 genome RNA was isolated using Trizol reagent (Invitrogen) according to manufacturer's instruction. To obtain cDNA, reverse transcription reaction was done using the RevertAid H Minus First Strand cDNA Synthesis kit. Appropriate fragment of gp41 cDNA containing sequence recognized by HRz-gp41, TLR-HRz-gp41 and Dz-gp41 was prepared by PCR amplification using as a template 1 µl of reverse transcription mixture per 10 µl of PCR reaction mixture volume. Restriction sites for HindIII in forward primer and BamHI in reverse primer (shown in bold) were included as follows: forward- 5′ AT**AAGC TT**GAGCAGCAGGAAGCA 3′, reverse- AT**GGATCC**CAC TCCATCCAGGT. The 323-nt PCR-amplified fragment was purified on 1.5% agarose gel and electroeluted for 20–30 min at 83 mA. Next, the DNA ends were digested by HindIII and BamHI to prepare the fragment to clone into the pEGFP-N3 vector (Clontech). To duplicate pEGFP-N3-gp41-323 construct, DH5α *Escherichia coli* bacterial strain was used as a host for the transformation. Length and orientation of the cloned product were verified by DNA sequencing, using femtomole DNA Sequencing System (Promega). For human cells, transfection experiments the pEGFP-N3-gp41-323 plasmid was isolated and purified from transformants using Perfectprep Plasmid Midi Kit (Eppendorf).

Cell Cultures and Transfection—Human HeLa cells were seeded at a density 2×10^5 cells per well in 24-well tissue culture plates (Nunc) and grown in RPMI 1640 medium (Sigma) with 10% fetal bovine serum (FBS; Gibco), 1% antibiotics (Sigma) and 1% RPMI vitamins mix (Sigma) at 37°C under 5% CO_2 atmosphere. After 1 day, cells were washed with phosphate-buffered saline (Sigma), placed in fresh RPMI-1640 medium without supplements and co-transfected with 1 µg pEGFP-N3-gp41-323 and catalytic nucleic acids to final concentrations of 10, 25, 50 and 100 nM. Transfections were done in the presence of 1.5 µl Lipofectamine 2000 (Invitrogen) with 500 µl Opti-MEM (Invitrogen) following the manufacturer's protocol. After 4 h, medium was replaced with fresh RPMI-1640 medium with supplements and cells were incubated for 24 h at 37°C under 5% CO_2 atmosphere. Total RNA was isolated using Trizol reagent (Invitrogen).

RT–PCR Analysis—The level of gp41 expression inhibition was analysed using RT–PCR. For reverse transcription, we used 1–2 µg of total RNA, hexamer random primers and RevertAid™ H Minus First Strand cDNA Synthesis Kit (Fermentas). An aliquot of cDNA was used for PCR amplification with *Taq* polymerase (Fermentas) and gp41-specific primers: gp41-A: 5′-CTTGGGTTCTTGGGAGCAGC-3′ and gp41-B: 5′-GTATTCCAAGGCACAGCAGTG-3′ as well as GAPDH primers as an internal control. Equal volumes of PCR reaction mixtures were analysed on 1.5% agarose gels, stained with ethidium bromide and quantified using Typhoon 8600 Imager with ImageQuant software.

RESULTS

Design of the Catalytic Nucleic Acids—The HH ribozymes and the DNAzyme used in this study were designed to recognize and cleave a GUA-containing sequence 1580 nucleotides downstream from the HIV-1 envelope glycoproteins (*env*) gene initiation codon. The choice of a target sequence in design of antiviral antisense oligonucleotides and catalytic RNAs is particularly crucial in the case of HIV which shows a high nucleotide sequence variations between strains. The target sequence was selected based on the comparison of gp41-coding sequences available from the GenBank. The region targeted by DNA and ribozymes used in this study is well conserved and can constitute a universal target with 95% conservation of the GUA triplet at the cleavage site.

The HH ribozymes targeting gp41-coding sequence were prepared in two versions. The minimal ribozyme (HRz-gp41) consisted of the catalytic core and 6-nt long sequences complementary to the target site (Fig. 1A). The second ribozyme (TLR-HRz-gp41) contained 5′-terminal extension with a TLR motif to bind a GAAA TL within the ribozyme's catalytic core. To increase the RNA's stability, we introduced six LNA analogs in the 5′- and 3′-terminal sequences of the construct (Fig. 1B). The third catalytic nucleic acid used in this study was a DNAzyme (Dz-gp41) targeted at the same site as the HH ribozymes (Fig. 1C). As negative controls we used constructs carrying mutations within catalytic cores (Fig. 1A–C).

Catalytic Activity of the Ribozymes and DNAzyme—The effect of magnesium on the cleavage reaction was analysed at increasing concentration of $MgCl_2$ (Fig. 2). The specific cleavage of the substrate was observed at A13 for HRz-gp41 and TLR-HRz-gp41 and at G11 for Dz-gp41. All constructs cleaved the substrate in a whole spectrum (0.1–25 mM) of magnesium concentrations, but with different efficiency. The most effective catalyst was the extended TLR-HRz-gp41 ribozyme with TL-TLR stabilizing motif (Fig. 2C). This ribozyme was very active even at low magnesium concentrations. The reaction yield at 1mM $MgCl_2$ was almost 20%, while much higher (over 10 mM) concentration of magnesium was required for comparable results with the minimal ribozyme HRz-gp41. At 1 mM $MgCl_2$, HRz-gp41 activity was only 6%. Increasing Mg^{2+} concentration resulted in higher yield of hydrolysis of all catalytic nucleic acids. At 10 mM $MgCl_2$, we observed 60% and 20% of cleaved substrate with TLR-HRz-gp41 and HRz-gp41, respectively. The 10–23

DNAzyme (Dz-gp41) shows higher activity than the minimal HRz-gp41 ribozyme, reaching 10% and 51% at 1 and 10 mM $MgCl_2$, respectively, but not as high as the TLR-HRz-gp41 (Fig. 2C).

Based on its superior performance, TLR-HRz-gp41 (Fig. 1B) was selected for further experiments. We examined an influence of TLR-HRz-gp41 concentration on gp41-25 substrate hydrolysis in the presence of 0.5 and 10 mM of $MgCl_2$. Increasing ribozyme to substrate ratio resulted in a higher yield of hydrolysis reaction. At 100-fold excess of ribozyme in 0.5 and 10 mM magnesium, the reaction yields were over 30% and over 80%, respectively (Fig. 3, Supplementary Fig. S1). TLR-HRz-gp41 also shows high efficiency at low magnesium concentrations. Reactions carried out in the presence of 0.5 and 1 mM $MgCl_2$ for 60 min resulted in over 50% and over 70% hydrolysis (Fig. 4). The constructs with mutations within catalytic cores MHRz-gp41, MTLR-HRz-gp41 and MDz-gp41 (Fig. 1) assayed at 10 mM $MgCl_2$/pH 7.5/25°C with gp41-25 substrate were found to be inactive (Supplementary Fig. S2).

Kinetics of the Ribozyme and DNAzyme Catalyzed Cleavage—The cleavage rate constants were determined for all catalytically active nucleic acids used in this study (Table 1). The reactions were carried out at 100-fold excess ribozyme (1 μM) over substrate (10 nM). For TLR-HRz-gp41, HRz-gp41 and Dz-gp41, the observed cleavage rate constants (k_{obs}) measured at 10 mM $MgCl_2$. were 1.456, 0.321 and 0.812 min^{-1}, respectively. The TLR-HRz-gp41 was assayed at 0.5 and 1 mM $MgCl_2$ and revealed k_{obs} of 0.057 and 0.136 min^{-1}, respectively.

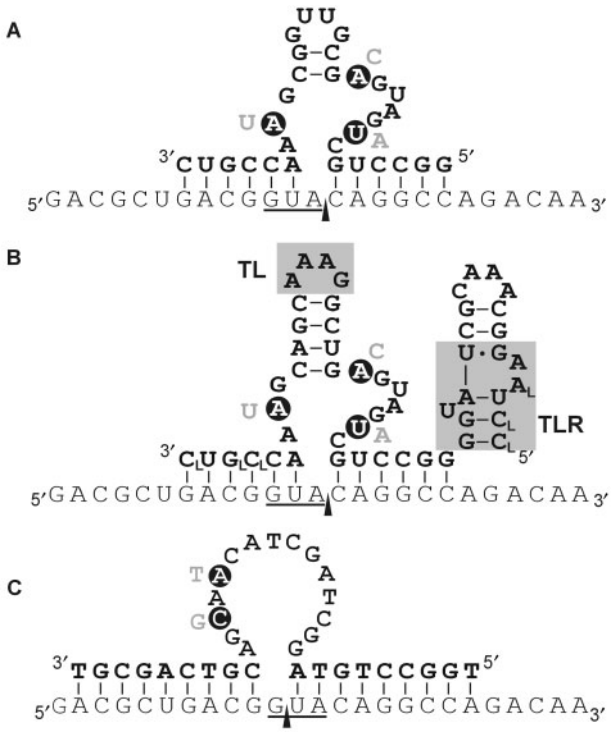

Fig. 1. **Catalytic nucleic acids used in the study.** Catalytic strands are shown in bold and target sequences in the substrate are underlined. Arrows indicate cleavage sites. (A) Minimal HH ribozyme HRz-gp41. (B) Extended HH ribozyme TLR-HRz-gp41. The GAAA TL and a TLR motif are shown in shaded boxes. LNA modifications in the TLR-HRz-gp41$_{LNA}$ are marked with subscript L. (C) A DNAzyme '10–23' Dz-gp41. Nucleotides substituted in mutant constructs MHRz-gp41, MTLR-HRz-gp41 and MDz-gp41 are shown in black circles.

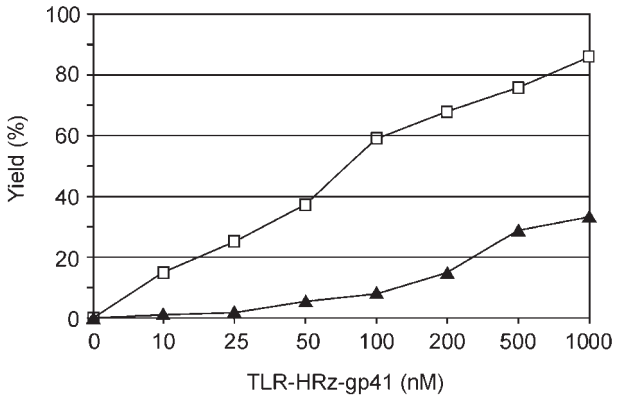

Fig. 3. **Catalytic activity of TLR-HRz-gp41 in increasing concentration.** A plot of *in vitro* hydrolytic activity of TLR-HRz-gp41 depending on its concentration in the presence of 0.5 mM (triangles) and 10 mM $MgCl_2$ (squares). A 10 nM of gp41-25 was cleaved with 10, 25, 50, 100, 200, 500 and 1000 nM TLR-HRz- gp41. Reactions were carried out in 50 mM Tris–HCl buffer pH 7.5, at 25°C for 30 min.

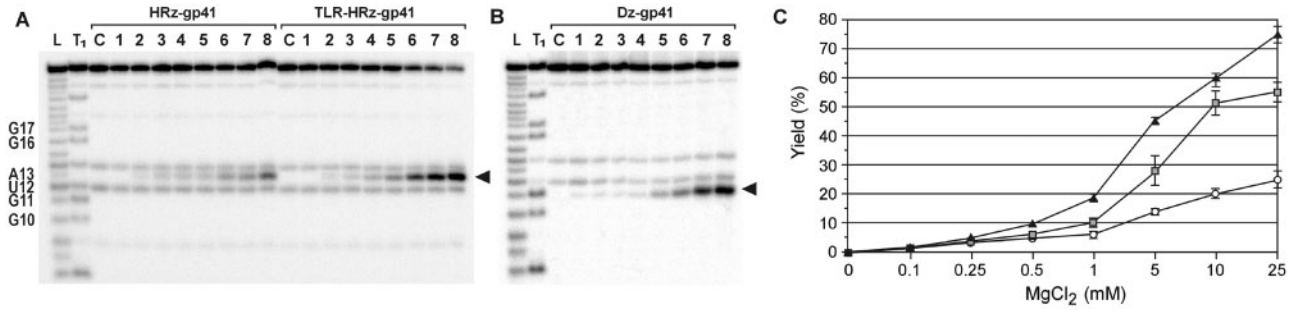

Fig. 2. ***In vitro*** **activity of HRz-gp41, TLR-HRz-gp41 and Dz-gp41 depending on Mg^{2+} concentration.** A 10 nM of gp41-25 was cleaved with 100 nM HRz-gp41or TLR-HRz-gp41 (A) and Dz-gp41 (B) for 30 min at increasing concentrations of $MgCl_2$ (0–25 mM). L, ladder; T1, limited hydrolysis with RNase T_1; C, control; 1–8, cleavage reactions in the presence of 0, 0.1, 0.25, 0.5, 1, 5, 10 and 25 mM $MgCl_2$, respectively. Arrows indicate the cleavage product. (C) A plot of hydrolytic activity of HRz-gp41 (circles), TLR-HRz-gp41 (triangles) and Dz-gp41 (squares) depending on magnesium ions concentration.

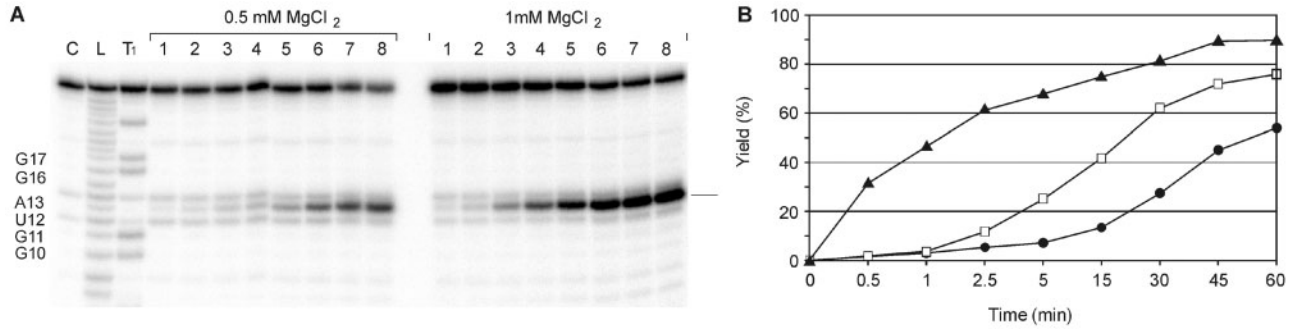

Fig. 4. **The effect of reaction time on the gp41-25 cleavage with TLR-HRz-gp41.** (A) Time dependence of *in vitro* hydrolysis of 10 nM gp41-25 with 1μM TLR-HRz-gp41. Lanes: C, control; L, ladder; T1, limited hydrolysis RNase T_1; 1–8, hydrolysis of gp41-25 in presence of TLR-HRz-gp41 for 0.5, 1, 2.5, 5, 15, 30, 45 and 60 min, respectively. Arrow shows the cleavage product. (B) A plot of hydrolytic activity of TLR-HRz-gp41 depending on incubation time in the presence of 0.5 mM (circles), 1 mM (squares) and 10 mM $MgCl_2$ (triangles).

Table 1. **Kinetic parameters of catalytic nucleic acids targeted in gp41 mRNA of HIV-1.**

		Reaction conditions			
		Excess of catalytic nucleic acids		Excess of gp41-25 substrate	
Catalytic nucleic acid	$MgCl_2$ [mM]	K_{obs} (min^{-1})	Error	K_{obs} (min^{-1})	Error
TLR-HRz-gp-41	10	1.456	±0.129	4×10^{-2}	$\pm 10^{-2}$
TLR-HRz-gp-41	1	0.136	±0.025	3.48×10^{-3}	$\pm 5.5 \times 10^{-4}$
TLR-HRz-gp-41	0.5	0.057	±0.004	2.31×10^{-3}	$\pm 5.1 \times 10^{-4}$
TLR-HRz-gp-41$_{LNA}$	10	1.461	±0.360	n/d	n/d
Dz-gp-41	10	0.812	±0.014	n/d	n/d
HRz-gp-41	10	0.321	±0.017	n/d	n/d

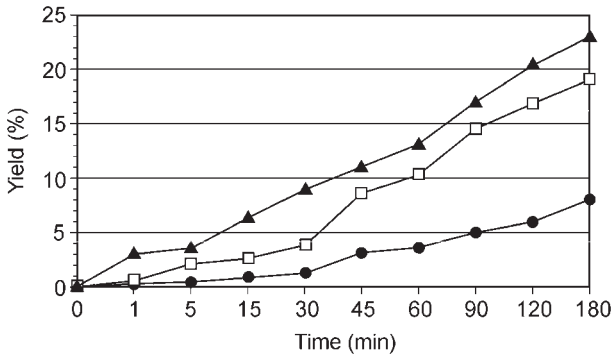

Fig. 5. **Hydrolytic activity of TLR-HRz-gp41 at 10-fold excess of substrate.** Time-dependent hydrolysis of 100 nM of gp41-25 with 10 nM TLR-HRz-gp41 was carried out at in the presence of 0.5 mM (circles), 1 mM (squares) and 10 mM $MgCl_2$ (triangles).

The influence of magnesium on the catalytic properties of TLR-HRz-gp41 was also analysed using excess of the substrate. The reactions contained 10 nM TLR-HRz-gp41 and 100 nM of gp41-25 RNA in buffers with 0.5, 1 and 10 mM $MgCl_2$ (Fig. 5) and showed K_{obs} values of 0.231×10^{-2}, 0.348×10^{-2} and $0.04\,min^{-1}$, respectively (Table 1). An analysis of the influence of increasing substrate/ribozyme ratio on the activity of TLR-HRz-gp41 at 10 mM $MgCl_2$ for 30 min showed efficient cleavage in the whole range of concentrations (10–500 nM) (Supplementary Fig. S3).

Stability and Activity of LNA-modified HH Ribozyme— To increase the stability of the TLR-HRz-gp41 ribozyme, we introduced LNA modifications at 5′- and 3′-ends (Fig. 1B). LNA-modified RNA is significantly more resistant to nucleolytic degradation in HeLa cell extract than unmodified RNA (Supplementary Fig. S4). The modified ribozyme shows similar catalytic properties as its unmodified counterpart with the observed cleavage rate constant (k_{obs}) at 10 mM $MgCl_2$of $1.46\,min^{-1}$ (Table 1).

Activity of Ribozymes and DNAzyme in HeLa Cells— The ribozymes and the DNAzyme were tested in cultured cells. HeLa cells were co-transfected with pEGFP-N3-323 vector containing target sequence and several concentrations of ribozymes and DNAzyme (10, 25, 50 and 100 nM) in the presence of Lipofectamine 2000. The activities of catalytic nucleic acids were estimated 24 h after transfection as an inhibition of gp41-green fluorescent protein (GFP) fusion protein expression observed as a decrease in the intensity of fluorescence from the GFP (Fig. 6). These experiments demonstrated that the most effective silencing factors were TLR-stabilized ribozymes TLR-HRz-gp41 and TLR-HRz-gp41$_{LNA}$. The efficiency of HH ribozymes and DNAzyme was further analysed in detail using RT–PCR with the primers flanking the target site within chimeric GFP-gp41 gene (Supplementary Fig. S5). The co-transfection of gp41-GFP fusion protein encoding plasmid with the catalytic nucleic acids resulted in a dose-dependent decrease of the intact gp41-GFP mRNA.

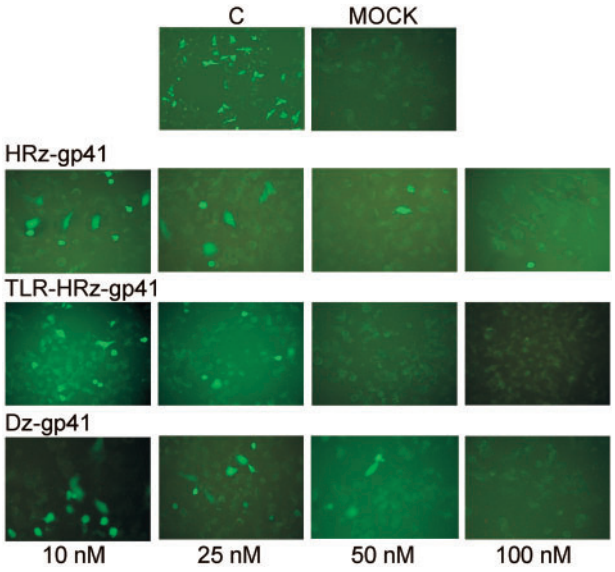

Fig. 6. **Silencing of HIV-1 gp41-GFP reporter gene in HeLa cells.** Cells were co-transfected with 1 μg pEGFP-N3-gp41-323 and 10, 25, 50 and 100 nM of catalytic nucleic acids. C, cells transfected with pEGFP-N3-gp41-323 alone; MOCK, untreated cells; HRz-gp41, TLR-HRz-gp41, Dz-gp41-cells cotransfected with pEGFP-N3-gp41-323 and appropriate catalytic constructs. Pictures were taken 24 h after transfection and represent fragment of the overall microscopic view.

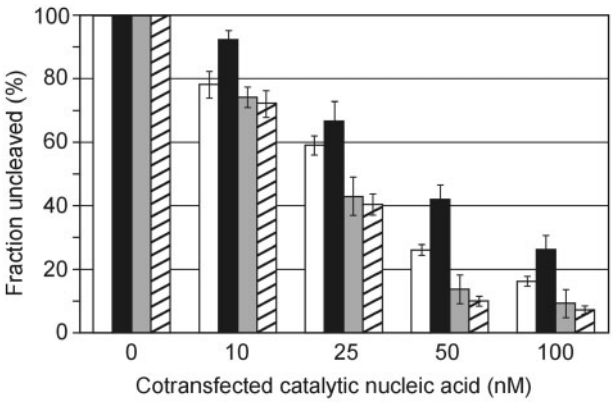

Fig. 7. **HIV-1 gp41-GFP mRNA silencing by catalytic nucleic acids.** A plot of dose-dependent inhibition of gp41-GFP mRNA expression with HRz-gp41 (white bars), Dz-gp41 (black bars), TLR-HRz-gp41 (grey bars) and TLR-HRz-gp41$_{LNA}$ (striped bars) in co-transfected HeLa cells.

The most effective molecule was TLR-HRz-gp41. Quantitative analysis revealed that the addition of 25 and 50 nM of TL-TLR-stabilized ribozymes resulted in 60% and 90% reduction of the amount of GFP-gp41 mRNA (Fig. 7). Although, the LNA-modified ribozyme was shown to be more stable in HeLa cells extract we did not observe significant differences in the silencing effect between TLR-HRz-gp41 and TLR-HRz-gp41$_{LNA}$ in the cells.

DISCUSSION

One of the major obstacles in application of catalytic RNAs as therapeutic agents is a high concentration of magnesium required for their activity. *In vitro*, ribozymes show the highest efficiency in buffers containing over 10 mM Mg^{2+}. In recent years, it has been demonstrated that, contrary to earlier beliefs, divalent ions do not participate directly in the catalysis, but stabilize a higher order structure of RNA. It is required for proper conformation of the active site that facilitates hydrolytic cleavage of target RNA (*39*, *40*). However, intracellular concentration of magnesium is much lower than that required for the HH ribozyme activity *in vitro*. Thus, the primary objective in design of novel catalytic RNAs is lowering their Mg^{2+} requirement, while retaining a high enzymatic activity. One of the HH ribozyme variants active at low magnesium has been obtained using *in vitro* selection technique by shortening stem-loop II (*38*). Another way of improving HH ribozyme efficiency at low Mg^{2+} concentrations is an increase of structure stability through tertiary interactions between stems I and II, mimicking a conformation of naturally occurring ribozymes (*37*, *41*). It has been demonstrated that structural motifs of the naturally occurring HH ribozymes of Tobacco Ring-Spot Virus satellite RNA (sTRSV) or artificially selected sequences capable of forming tertiary interactions between helices I and II improve catalytic activity of ribozymes *in vitro* at submillimolar concentrations of magnesium ions.

In our attempts to obtain an efficient HH ribozyme against a target sequence within the mRNA encoding HIV-1 glycoprotein gp41, we took advantage of the highly specific tertiary RNA structure element consisting of the GAAA TL that is a part of the minimal ribozyme motif and a TLR attached to the 5′-end of the construct. We assume that the docking of the TL to its receptor stabilizes active conformation of the ribozyme's catalytic core in a similar manner as in the naturally occurring HH ribozyme motifs. Although the GNRA TLRs have not been found as natural stabilizing elements in HH ribozymes it provides a well defined and highly specific motif involved in establishing long-range tertiary interactions and proper folding of large RNA molecules. GAAA TLs that bind the receptor domain are evolutionarily conserved in group I and II introns and RNase P RNAs in bacteria (*42*) and they play a pivotal role in spatial organization of RNA required for catalysis (*43*).

The most important factor determining the usefulness of the GAAA TL and TLR for stabilizing RNA structure is a fact that their interaction does not require divalent ions. Although, it has been shown that magnesium increases the strength of interaction between the TL and receptor it is not absolutely required for the docking to take place. Within the range of 0–10 mM Mg^{2+}, there is ~40-fold increase in the binding force, but even without magnesium a loop–receptor complex can form (*44*). This suggests that divalent ions are not required for the interaction itself, but rather play a stabilizing role. Such a notion was also confirmed by recent NMR studies on the distribution of metal ions in the structure of GAAA TL–receptor complexes (*45*).

In vitro assays with a short, 25-nt long, substrate demonstrated that the TL–TLR stabilized ribozyme (TLR-HRz-gp41) shows higher catalytic activity than the minimal ribozyme (HRz-gp41) with the same sequence. The yield of the reaction was 3-fold higher for TLR-HRz-gp41 than for HRz-gp41. Although, the efficiency of hydrolysis catalysed by TLR-HRz-gp41 was dependent on the magnesium concentration, it still retained high activity at submillimolar levels of Mg^{2+}. Remarkably, at identical conditions, the activity of TLR-HRz-gp41 was higher than that of the DNAzyme targeting the same sequence. The cleavage rate constants in single turnover reaction, measured at 10 mM Mg^{2+} for TLR-HRz-gp41 were 4.5- and 1.8-fold higher than for HRz-gp41 and DNAzyme, respectively. At 1 mM and 0.5 mM magnesium concentration, we observed 10- and 20-fold decrease in the cleavage rate which is consistent with the stabilizing effect of divalent ions on both overall structure of RNA and the tertiary interactions between TL and receptor motifs.

Another important issue that has to be addressed for the efficient application of RNA technologies *in vivo* is a susceptibility of RNA molecules to degradation. One of the methods used to increase the stability of RNA *in vivo* is an introduction of nucleotide analogues that enhance RNA's resistance against ribonucleases. It has been demonstrated that extensively modified HH ribozymes in which ribonucleotides have been substituted by 2′-*O*-methyl and 2′-*O*-allyl analogues show increased stability in serum and retain high enzymatic activity (*46*). In recent years, a new family of nucleotide analogues was developed. LNA represent conformationally locked nucleotide analogues with improved affinity and nuclease resistance (*47*, *48*). Antisense oligonucleotides containing LNA analogues have been shown to possess a higher activity both *in vitro* and *in vivo*. Moreover, LNA-modified nucleic acids are virtually non-toxic (*49*). We demonstrated that TLR-HRz-gp41 construct in which six LNA nucleotide analogues are introduced within the 5′-terminal extension containing TLR motif and the 3′ target recognition sequence show increased stability in serum, while retaining its catalytic activity. The kinetic parameters of LNA-modified ribozyme were virtually identical to these of unmodified TRL-HRz-gp41. This result also suggests that the LNA modification of three nucleotides within the TLR motif have little or no effect on the docking of the GAAA TL. The modifications of three nucleotides within the terminal 3′ target recognition sequence also had no apparent effect on the catalytic activity.

The TLR containing ribozyme was also shown to be an efficient silencer of the of target gene expression in HeLa cells. When co-transfected with the plasmid carrying modified GFP gene containing gp41 fragment, TLR-HRz-gp41 efficiently interfered with the expression of GFP. RT–PCR demonstrated that the silencing effect is due to disruption of the GFP-gp41-encoding mRNA by ribozyme-catalysed hydrolysis. The extended ribozymes were more efficient in inhibition of GFP expression than minimal HH ribozyme and the DNAzyme, however, we did not observe significant difference between all-RNA and LNA-modified TLR-HRz-gp41 that could be expected from the observation of higher stability of TLR-HRz-$gp41_{LNA}$.

In summary, we demonstrate that the interaction of GAAA TL with TLR improves the catalytic activity of HH ribozymes. The ribozyme containing the TLR shows better kinetic parameters than the minimal HH motif and retains high activity at low magnesium concentrations. Docking of the TL to the receptor stabilizes active conformation of the ribozyme bringing together helices I and II. Lower magnesium requirement of the TL/TLR-stabilized ribozyme may also be responsible for its improved performance in the intracellular environment. In this report, we demonstrate for the first time that the ribozymes stabilized with tertiary interactions not only show better kinetic parameters *in vitro*, but also can be used for efficient silencing of gene expression in the cells.

Thus, the design of novel variants of HH ribozymes based on the tertiary interactions between specific TLs and respective receptor motifs seems to be a viable method for the improvement of their efficiency at physiological magnesium concentrations. The practical application of a rational design of RNA structures based on well-defined RNA–RNA recognition motifs was also demonstrated in the development of an artificial ribozyme showing RNA ligase activity (*50*). It has been demonstrated that GAAA TLs and TLRs can provide highly specific recognition elements for enzyme–substrate binding. Recently, *in vitro* selection methods have been used to develop new TLR variants that tightly bind to GGAA TL (*51*). It is therefore possible, that even more efficient ribozyme variants can be designed following the outlined principle.

SUPPLEMENTARY DATA

Supplementary data are available at *JB* online.

FUNDING

Polish Ministry of Science and Higher Education (N N302 220535).

CONFLICT OF INTEREST

None declared.

REFERENCES

1. Kruger, K., Grabowski, P.J., Zaug, A.J., Sands, J., Gottschling, D.E., and Cech, T.R. (1982) Self-splicing RNA: autoexcision and autocyclization of the ribosomal RNA intervening sequence of Tetrahymena. *Cell* **31**, 147–157
2. Guerrier-Takada, C., Gardiner, K., Marsh, T., Pace, N., and Altman, S. (1983) The RNA moiety of ribonuclease P is the catalytic subunit of the enzyme. *Cell* **35**, 849–857
3. Nelson, J.A. and Uhlenbeck, O.C. (2008) Hammerhead redux: does the new structure fit the old biochemical data? *RNA* **14**, 605–615
4. Sarver, N., Cantin, E.M., Chang, P.S., Zaia, J.A., Ladne, P.A., Stephens, D.A., and Rossi, J.J. (1990) Ribozymes as potential anti-HIV-1 therapeutic agents. *Science* **247**, 1222–1225
5. Sun, L.Q., Cairns, M.J., Saravolac, E.G., Baker, A., and Gerlach, W.L. (2000) Catalytic nucleic acids: from lab to applications. *Pharmacol. Rev.* **52**, 325–347

6. Stage-Zimmermann, T.K. and Uhlenbeck, O.C. (1998) Hammerhead ribozyme kinetics. *RNA* **4**, 875–889
7. Bruening, G. (1989) Compilation of self-cleaving sequences from plant virus satellite RNAs and other sources. *Methods Enzymol.* **180**, 546–558
8. Collins, R.F., Gellatly, D.L., Sehgal, O.P., and Abouhaidar, M.G. (1998) Self-cleaving circular RNA associated with rice yellow mottle virus is the smallest viroid-like RNA. *Virology* **241**, 269–275
9. Doudna, J.A. and Cech, T.R. (2002) The chemical repertoire of natural ribozymes. *Nature* **418**, 222–228
10. Citti, L. and Rainaldi, G. (2005) Synthetic hammerhead ribozymes as therapeutic tools to control disease genes. *Curr. Gene Ther.* **5**, 11–24
11. Khan, A.U. and Lal, S.K. (2003) Ribozymes: a modern tool in medicine. *J. Biomed. Sci.* **10**, 457–467
12. Ngok, F.K., Mitsuyasu, R.T., Macpherson, J.L., Boyd, M.P., Symonds, G.P., and Amado, R.G. (2004) Clinical gene therapy research utilizing ribozymes: application to the treatment of HIV/AIDS. *Methods Mol. Biol.* **252**, 581–598
13. Khan, A.U. (2006) Ribozyme: a clinical tool. *Clin. Chim. Acta* **367**, 20–27
14. Lustig, B. and Jeang, K.T. (2001) Biological applications of hammerhead ribozymes as anti-viral molecules. *Curr. Med. Chem.* **8**, 1181–1187
15. Schubert, S. and Kurreck, J. (2006) Oligonucleotide-based antiviral strategies. *Handb. Exp. Pharmacol.* **173**, 261–287
16. Hotchkiss, G., Maijgren-Steffensson, C., and Ahrlund-Richter, L. (2004) Efficacy and mode of action of hammerhead and hairpin ribozymes against various HIV-1 target sites. *Mol. Ther.* **10**, 172–180
17. Rossi, J.J. (2000) Ribozyme therapy for HIV infection. *Adv. Drug Deliv. Rev.* **44**, 71–78
18. Frankel, A.D. and Young, J.A. (1998) HIV-1: fifteen proteins and an RNA. *Annu. Rev. Biochem.* **67**, 1–25
19. Turner, B.G. and Summers, M.F. (1999) Structural biology of HIV. *J. Mol. Biol.* **285**, 1–32
20. Eckert, D.M. and Kim, P.S. (2001) Mechanisms of viral membrane fusion and its inhibition. *Annu. Rev. Biochem.* **70**, 777–810
21. Ebenbichler, C.F., Thielens, N.M., Vornhagen, R., Marschang, P., Arlaud, G.J., and Dierich, M.P. (1991) Human immunodeficiency virus type 1 activates the classical pathway of complement by direct C1 binding through specific sites in the transmembrane glycoprotein gp41. *J. Exp. Med.* **174**, 1417–1424
22. Wang, H., Nishanian, P., and Fahey, J.L. (1995) Characterization of immune suppression by a synthetic HIV gp41 peptide. *Cell. Immunol.* **161**, 236–243
23. Akridge, R.E., Oyafuso, L.K., and Reed, S.G. (1994) IL-10 is induced during HIV-1 infection and is capable of decreasing viral replication in human macrophages. *J. Immunol.* **153**, 5782–5789
24. Ameglio, F., Cordiali Fei, P., Solmone, M., Bonifati, C., Prignano, G., Giglio, A., Caprilli, F., Gentili, G., and Capobianchi, M.R. (1994) Serum IL-10 levels in HIV-positive subjects: correlation with CDC stages. *J. Biol. Regul. Homeost. Agents* **8**, 48–52
25. Rosenberg, Z.F. and Fauci, A.S. (1990) Immunopathogenic mechanisms of HIV infection: cytokine induction of HIV expression. *Immunol. Today* **11**, 176–180
26. Klein, S.A., Dobmeyer, J.M., Dobmeyer, T.S., Pape, M., Ottmann, O.G., Helm, E.B., Hoelzer, D., and Rossol, R. (1997) Demonstration of the Th1 to Th2 cytokine shift during the course of HIV-1 infection using cytoplasmic cytokine detection on single cell level by flow cytometry. *AIDS* **11**, 1111–1118
27. Merrill, J.E., Koyanagi, Y., Zack, J., Thomas, L., Martin, F., and Chen, I.S. (1992) Induction of interleukin-1 and tumor necrosis factor alpha in brain cultures by human immunodeficiency virus type 1. *J. Virol.* **66**, 2217–2225
28. Koka, P., He, K., Zack, J.A., Kitchen, S., Peacock, W., Fried, I., Tran, T., Yashar, S.S., and Merrill, J.E. (1995) Human immunodeficiency virus 1 envelope proteins induce interleukin 1, tumor necrosis factor alpha, and nitric oxide in glial cultures derived from fetal, neonatal, and adult human brain. *J. Exp. Med.* **182**, 941–951
29. Chen, Y.H., Christiansen, A., and Dierich, M.P. (1995) HIV-1 gp41 selectively inhibits spontaneous cell proliferation of human cell lines and mitogen- and recall antigen-induced lymphocyte proliferation. *Immunol. Lett.* **48**, 39–44
30. Barcova, M., Kacani, L., Speth, C., and Dierich, M.P. (1998) gp41 envelope protein of human immunodeficiency virus induces interleukin (IL)-10 in monocytes, but not in B, T, or NK cells, leading to reduced IL-2 and interferon-gamma production. *J. Infect. Dis.* **177**, 905–913
31. Koutsonikolis, A., Haraguchi, S., Brigino, E.N., Owens, U.E., Good, R.A., and Day, N.K. (1997) HIV-1 recombinant gp41 induces IL-10 expression and production in peripheral blood monocytes but not in T-lymphocytes. *Immunol. Lett.* **55**, 109–113
32. Adamson, D.C., Wildemann, B., Sasaki, M., Glass, J.D., McArthur, J.C., Christov, V.I., Dawson, T.M., and Dawson, V.L. (1996) Immunologic NO synthase: elevation in severe AIDS dementia and induction by HIV-1 gp41. *Science* **274**, 1917–1921
33. Speth, C., Joebstl, B., Barcova, M., and Dierich, M.P. (2000) HIV-1 envelope protein gp41 modulates expression of interleukin-10 and chemokine receptors on monocytes, astrocytes and neurones. *AIDS* **14**, 629–636
34. London, R.E. (1991) Methods for measurement of intracellular magnesium: NMR and fluorescence. *Annu. Rev. Physiol.* **53**, 241–258
35. Romani, A. and Scarpa, A. (1992) Regulation of cell magnesium. *Arch. Biochem. Biophys.* **298**, 1–12
36. Uetani, T., Matsubara, T., Nomura, H., Murohara, T., and Nakayama, S. (2003) Ca^{2+}-dependent modulation of intracellular Mg2+ concentration with amiloride and KB-R7943 in pig carotid artery. *J. Biol. Chem.* **278**, 47491–47497
37. Burke, D.H. and Greathouse, S.T. (2005) Low-magnesium, trans-cleavage activity by type III, tertiary stabilized hammerhead ribozymes with stem 1 discontinuities. *BMC Biochem.* **6**, 14
38. Persson, T., Hartmann, R.K., and Eckstein, F. (2002) Selection of hammerhead ribozyme variants with low Mg^{2+} requirement: importance of stem-loop II. *Chembiochem* **3**, 1066–1071
39. Nelson, J.A. and Uhlenbeck, O.C. (2008) Minimal and extended hammerheads utilize a similar dynamic reaction mechanism for catalysis. *RNA* **14**, 43–54
40. Fedoruk-Wyszomirska, A., Wyszko, E., Giel-Pietraszuk, M., Barciszewska, M.Z., and Barciszewski, J. (2007) High hydrostatic pressure approach proves RNA catalytic activity without magnesium. *Int. J. Biol. Macromol.* **41**, 30–35
41. Saksmerprome, V., Roychowdhury-Saha, M., Jayasena, S., Khvorova, A., and Burke, D.H. (2004) Artificial tertiary motifs stabilize trans-cleaving hammerhead ribozymes under conditions of submillimolar divalent ions and high temperatures. *RNA* **10**, 1916–1924
42. Costa, M. and Michel, F. (1995) Frequent use of the same tertiary motif by self-folding RNAs. *EMBO J.* **14**, 1276–1285
43. Cate, J.H., Gooding, A.R., Podell, E., Zhou, K., Golden, B.L., Kundrot, C.E., Cech, T.R., and Doudna, J.A. (1996) Crystal structure of a group I ribozyme domain: principles of RNA packing. *Science* **273**, 1678–1685
44. Hodak, J.H., Downey, C.D., Fiore, J.L., Pardi, A., and Nesbitt, D.J. (2005) Docking kinetics and equilibrium of a GAAA tetraloop-receptor motif probed by single-molecule FRET. *Proc. Natl Acad. Sci. USA* **102**, 10505–10510
45. Davis, J.H., Foster, T.R., Tonelli, M., and Butcher, S.E. (2007) Role of metal ions in the tetraloop-receptor complex as analyzed by NMR. *RNA* **13**, 76–86

46. Paolella, G., Sproat, B.S., and Lamond, A.I. (1992) Nuclease resistant ribozymes with high catalytic activity. *EMBO J.* **11**, 1913–1919
47. Braasch, D.A. and Corey, D.R. (2001) Locked nucleic acid (LNA): fine-tuning the recognition of DNA and RNA. *Chem. Biol.* **8**, 1–7
48. Grunweller, A., Wyszko, E., Bieber, B., Jhnel, R., Erdmann, V.A., and Kurreck, J. (2003) Comparison of different antisense strategies in mammalian cells using locked nucleic acids, 2′-O-methyl RNA, phosphorothioates and small interfering RNA. *Nucleic Acids Res.* **31**, 3185–3193
49. Wahlestedt, C., Salmi, P., Good, L., Kela, J., Johnsson, T., Hökfelt, T., Broberger, C., Porreca, F., Lai, J., Ren, K., Ossipov, M., Koshkin, A., Jakobsen, N., Skouv, J., Oerum, H., Jacobsen, M.H., and Wengel, J. (2000) Potent and nontoxic antisense oligonucleotides containing locked nucleic acids. *Proc. Natl Acad. Sci. USA* **97**, 5633–5638
50. Ikawa, Y., Tsuda, K., Matsumura, S., and Inoue, T. (2004) De novo synthesis and development of an RNA enzyme. *Proc. Natl Acad. Sci. USA* **101**, 13750–13755
51. Geary, C., Baudrey, S., and Jaeger, L. (2008) Comprehensive features of natural and in vitro selected GNRA tetraloop-binding receptors. *Nucleic Acids Res.* **36**, 1138–1152